Available online at http://scik.org

Commun. Math. Biol. Neurosci. 2025, 2025:2

https://doi.org/10.28919/cmbn/8924

ISSN: 2052-2541

IMPLICIT NUMERICAL APPROACH FOR BIOLOGICAL SCHNAKENBERG MODEL EMPLOYING FINITE ELEMENT METHOD (FEM)

NEK MUHAMMAD KATBAR[1,2,*], KHUDA BUX AMUR[3], ISRAR AHMED[4], IHSAN A. KHOSO[5,*], DARSHAN MAL[4], ABDUL HAKEEM[1], GHULAM ABBASS[1]

[1]School of Mathematics and Statistics, Central South University, Changsha 410083, China

[2]Mehran University of Engineering &Technology SZAB, Campus Khairpur Mir's, Sindh, Pakistan

[3]Department of Mathematics & Statistics, Quaid-e-Awam University of Engineering, Science & Technology, Nawabshah, Pakistan

[4]School of Mathematics Shah Abdul Latif University Khairpur Mir's, Sindh, Pakistan

[5]School of Electronic Engineering and Automation, Guilin University of Electronic Technology, Guilin 541004, China

Abstract. Finite Element Method (FEM) based numerical techniques for two-dimensional and two-directional problems are challenging for numerical analysis practitioners. In this study, an implicit numerical scheme was developed to solve a set of coupled non-linear partial differential equations using the finite element method. This study presents a numerical approach using Finite Element Method (FEM) to implicitly solve the Schnakenberg biological model. This method uses the inherent advantages of the finite element method, such as its adaptability and ability to deal with complex geometries, while also introducing a strategy to improve stability. A system of algebraic equations is derived from the model equations to compute spatiotemporal dynamics by discretizing the spatial domain. The numerical solution is obtained by iteratively solving the resulting algebraic equations, by employing suitable linear solvers and convergence criteria. The results also demonstrate that this method captures intricate spatial patterns of morphogenesis concentration in animal species. Furthermore, the objective of this study is to analyze stripe and spot-like patterns during morphogenesis in animal species.

*Corresponding authors

E-mail addresses: nekmuhammad@csu.edu.cn, ihsankhoso@gmail.com

Received October 06, 2024

Keywords: finite element method; Schnakenberg model; reaction-diffusion equations; morphogenesis; pattern formation; mathematical modeling.

2020 AMS Subject Classification: 92C15.

1. INTRODUCTION

Mathematical modeling is the process of describing real-life problems using mathematical ideas, symbols, and concepts. Modeling is an application of mathematics to real-world problems. A mathematical representation of a biological system is known as a biological model. To predict the future state of a system, it is necessary to model biological phenomena mathematically. Biological models have recently attracted significant attention [1]-[5]. Biological models are used to understand ecosystems, living beings, and other processes. Numerical models have been developed through mathematical modeling of biological phenomena, and spatial and temporal patterns have been derived in [6]. From a biological perspective, these patterns can be classified into two groups: chemical interaction and cell movement models. Gradient and reaction models are two subcategories. Pattern formation in biological modeling is associated with the diffusion or reaction of substances within a specific geometric configuration. The Schnakenberg model has been widely used as powerful model in numerous biological processes. This is an autocatalytic reaction that occurs in various biological models. During such reactions, the reaction rate increases as reaction proceeds. The authors proposed a scheme for solving the fractional- order Schnakenberg model and described an auto- chemical reaction with possible oscillatory behavior that may have several applications in biology and biochemistry [7]. Semi-analytical solutions for the Schnakenberg model in a reaction-diffusion cell with feedback mechanism and stability were examined in [8]. Faiz Muhammad Khan et al. developed an approximation scheme for fractional-order chemical Brusselator models using the widely used LADM [9]. Modeling multidimensional dynamical systems with partial differential equations (PDEs) is often used to formulate natural phenomena, such as heat, electrodynamics, quantum mechanics, and fluid dynamics [10][11]. O. Nikan et al. developed a localized mesh less algorithm for calculating the solution to a nonlinear biological population model (NBPM). The model describes the dynamics

of the biological population and makes valuable predictions under a variety of scenarios. Local radial basis functions (LRBF-PU) are used to approximate the solution to the NBPM [12][13]. Researchers have developed a method for analyzing the effects of initial conditions and growing domains on the competition between admissible modes in 3D truing pattern emergence using finite element modeling with Schnakenberg kinetics [14]. The Schnakenberg model is mathematical representation of reaction-diffusion processes that occur in biological systems, with two non-linear Partial Differential Equations (PDEs) that designate the temporal and spatial evolution of chemical concentrations. The model captures the dynamics of self-organization and pattern form, such as the distribution of morphogens during embryonic development, growth, and the development of biological systems, such as tumors or cell populations. Cell proliferation, migration, and interaction with surrounding tissue factors were also considered. Pattern formation phenomena commonly occur in biology and other sciences. The reaction and diffusion equations are used to model this phenomenon. The development of patterns in hydra [15], skin pigmentation, fish and tiger patterns, and butterfly wing pigmentation [16] are significant and interesting illustrations of the biological procedures of reaction-diffusion classifications. This is typically perceived when animal morphogenesis and skin pattern development occur [17][18]. Biological patterns can undergo generation, degradation, activation, or deactivation within the framework of image-guided biological systems [19]. Reaction diffusion equations can delineate diverse spatial patterns owing to the small-scale instabilities of chemical concentrations; this occurrence is referred to as diffusion unsteadiness [20][21]. The significance of many dynamic and biological existences in chemical theory, fluid dynamics, and mathematical biology lies in their ability to elucidate real-life processes. These phenomena are typically governed by non-linear partial differential equations (PDEs), which have the capacity to forecast dynamic occurrences worldwide and characterize exponential changes over time. PDEs determine widespread effectiveness across multiple domains, including physics, engineering, and biology, as researchers harness the power of differential equations to effectively model these systems [22]–[26]. Time-dependent nonlinear parabolic partial differential equations are numerically solved using the Modified Galerkin Weighted Residual Method (MGWRM) using modified

Bernstein polynomials. Using modified Bernstein polynomials, an approximate solution has been assumed. The modified Galerkin method was applied to transform the nonlinear parabolic PDEs into time-dependent ordinary differential equations [27]. The authors examined the solution of fractional partial differential equations of the parabolic type in Riesz space. Fractional-in-space operators have been successfully applied to mathematical physics problems, such as anomalous diffusion and dispersion and standard Brownian motion in terms of the Riesz derivative using the fractional order operator [28]. The Gray-Scott reaction-diffusion phenomenon has been extensively studied by eminent scholars [29]-[31]. Ali et al. [32] examined the Galerkin-Bernstein Approximations of the System of Time Dependent Nonlinear Parabolic PDE. A cubic B-spline has proven to be of considerable use to Mittal et al. [33], while assessing the model. Youssouf et al. solved the standard telegraph equation, a partial differential equation commonly used for modeling wave propagation in transmission lines, using the Laplace-Adomian method [34]. For many years reaction-diffusion systems have been used to gain deep insights into biological systems. Several chemical, biological, physical, and environmental processes have been modeled using these models in the real world. The most commonly used reaction-diffusion models are the Brusselator, Lengyel-Epstein, and Schnakenberg models because of their variety of applications and stability. Models of this type can be used to generate patterns in biological and chemical systems. In 1979, Schnakenberg familiarized himself with Schnakenberg's chemical reaction diffusion model. This model designates an auto-chemical reaction with oscillatory behavior, such as membrane investigation and embryogenesis. In addition, it also models the spatial distribution of the morphogen. The biological and physical behavior of tumor evolution in the presence of normal healthy tissue, considering various events involved in the process is investigated with mathematical formulation. These include hyper and hypoactivation of signaling pathways during tumor growth, vessels' growth, vascularization, and competition of cancer cells with healthy host tissue [35]. The Authors examined regression analysis and degree-based indices correlate with several physicochemical properties related to drug activities for heart attack. Various statistical parameters and Topological indices were used to analyze the Heart Attack drugs and other chemical properties [36][37]. The finite element method is a

powerful tool for numerical simulations of Biological and chemical systems. FEM is a numerical technique that is well suited for solving partial differential equations (PDEs) arising from various scientific and engineering problems. It discretizes the computational domain into smaller elements and approximates the solution within each element by using basis functions [38][39].

This study contributes to the field of mathematical biology by providing a robust and efficient numerical framework for studying the biological systems designated by the Schnakenberg model. Using diffuse flows and reaction rates, as well as boundary conditions, an implicit finite element method is used to investigate a variety of biological phenomena. Most computational strategies for solving problems of this type are based on finite difference methods, and rectangles are generally used as the discrete domain. We elucidated our problem using a triangular grid with local scaling diffusion parameters. The developed numerical scheme is applied to the Schnakenberg model. The purpose of this model was to calculate the morphogenesis concentration patterns for specific animal species.

2. PROBLEM FORMULATION

The Schnakenberg model is referred to as the morphogenesis model in the literature. Physiological morphogenesis refers to the growth and development of components according to their size, pattern, and physical structure. It can be used for pattern formation and morphogenic construction, such as bone formation, muscle formation, growth, and stability analysis. This model shows the behavior of a chemical activator denoted as u and a chemical inhibitor denoted as v.

Mathematically Schnakenberg model is given as follows

$$\begin{cases} \dfrac{\partial u}{\partial t} = \nabla^2 u + \lambda\, r(u,v) \\ \dfrac{\partial v}{\partial t} = \alpha \nabla^2 v + \lambda\, s(u,v) \end{cases} \tag{1}$$

The chemical species u is the activator and v is the inhibitor. $\nabla^2 u,\ \alpha \nabla^2 v$, is the diffusion term. The reaction relations are given as

$$\begin{cases} r(u,v) = c - u - u^2 v \\ s(u,v) = d - u^2 v \end{cases} \tag{2}$$

The terms $r(u,v)$ and $s(u,v)$ in Eq: (2) are reaction terms. λ, is the non-dimensional constant, c and d are constant production terms, and $u^2 v$ signifies the production term in the presence of inhibitor v. By substituting the values of the reaction terms, we obtain

$$\begin{cases} \dfrac{\partial u}{\partial t} = \nabla^2 u + \lambda(c - u + u^2 v), u \in \left[R^+ \times \Omega \right] \\ \dfrac{\partial v}{\partial t} = \alpha \nabla^2 v + \lambda (d - u^2 v) \quad , v \in \left[R^+ \times \Omega \right] \end{cases} \tag{3}$$

Using weighted residual

$$W.E = \int_{\Omega} w.E \, dx \tag{4}$$

The method of weighted residual yields

$$(\mathrm{W.E}) = 0 \tag{5}$$

Where

$$E = \begin{cases} \dfrac{\partial u}{\partial t} - \nabla^2 u - \lambda(c - u + u^2 v), u \in \left[R^+ \times \Omega \right] \\ \dfrac{\partial v}{\partial t} - \alpha \nabla^2 v - \lambda (d - u^2 v), v \in \left[R^+ \times \Omega \right] \end{cases} \tag{6}$$

The principle of variational formulation is to integrate the weighted residual into Ω . The variational formulation is as follows:

Let $u, v \in H^1(\Omega)$

$$\begin{cases} \displaystyle\int_{\Omega} s_1 \left(\frac{\partial u}{\partial t} - \nabla^2 u - \lambda(c - u + u^2 v) \right) d\Omega = 0 \\ \displaystyle\int_{\Omega} s_2 \left(\frac{\partial v}{\partial t} - \alpha \nabla^2 v - \lambda (d - u^2 v) \right) d\Omega = 0 \\ \text{for all } s_1, s_2 \in H^1(\Omega) \end{cases} \tag{7}$$

From Eq: (7) we obtain the following system

$$\begin{cases} Find\, u, v \in H^1(\Omega) \\ \int_\Omega \frac{\partial u}{\partial t} s_1 \, d\,\Omega - \int_\Omega \nabla^2 u \, s_1 \, d\,\Omega + \int_\Omega \lambda\,(c - u + u^2 v)\, s_1 d\,\Omega = 0 \\ \int_\Omega \frac{\partial v}{\partial t} s_2 \, d\,\Omega - \int_\Omega \alpha\, \nabla^2 v \, s_2 \, d\,\Omega + \int_\Omega \lambda\,(d - u^2 v)\, s_2 \, d\,\Omega = 0 \\ \forall s_1, s_2 \in H^1(\Omega) \end{cases} \tag{8}$$

Consider all boundary conditions assumed to be zero. Sobolev space is defined as

$$H^1(\Omega) = \left\{ u \in L^2(\Omega) : \nabla u \in (L^2(\Omega)) \right\} \tag{9}$$

Readers are recommended to review the basic theory of finite elements and Sobolev spaces for further details on Sobolev spaces in [40].

2.1. Discretization of the problem

Suppose Ω is a unit square domain (biological cell) and ζ_h is a family of triangles G with a maximum size $h > 0$. The discrete space X_h of continuous piecewise affine finite elements is considered over Ω as follows:

$$X_h = \left\{ s_h \in C^0(\bar{\Omega}) \mid \forall\, g \in \zeta_h, s_h \mid g \in P_1(G) \right\} \tag{10}$$

Where $X_h \subset X$ is the discrete space with P_1 finite points, and C^0 is a continuous space function. We considered triangular- grid ζ_h with each element h > 0. $P_1(G)$, shows spaces of one degree polynomial functions see ref [41]-[44]. As the problem is time- dependent, the next step is to discretize the time derivative.

We use the forward difference operators to discretize the time derivatives

$$\left\{ \begin{array}{ll} \frac{\partial u_h}{\partial t} & = \frac{{u_h}^{i+1} - {u_h}^{i}}{\Delta t} \\ \frac{\partial v_h}{\partial t} & = \frac{{u_h}^{i+1} - {u_h}^{i}}{\Delta t} \end{array} \right\} \tag{11}$$

$$\begin{cases} u_h, v_h \in H^1(\Omega) \\ \int_\Omega \left(\frac{{u_h}^{i+1} - {u_h}^{i}}{\Delta t}\right) s_{h1} \, d\Omega = -\int_\Omega \nabla u_h \nabla s_{h1} d\Omega - \lambda \int_\Omega u_h s_{h1} d\Omega + \int_\Omega \lambda (c + {u_h}^2 v_h) s_{h1} \, d\Omega \\ \int_\Omega \left(\frac{{v_h}^{i+1} - {v_h}^{i}}{\Delta t}\right) s_{h2} d\,\Omega = -\int_\Omega \alpha\, \nabla v_h \nabla s_{h2} d\,\Omega + \int_\Omega \lambda\,(d - {u_h}^2 v_h)\; s_{h2} d\,\Omega \\ \text{for all } s_{h1}, s_{h2} \in H^1(\Omega) \end{cases} \tag{12}$$

The linearization technique is used owing to the nonlinearity of the problem. The discretized form of (12) is as follows:

$$\begin{cases} u_h, v_h \in H^1(\Omega) \\ \int_\Omega (u_h{}^{i+1}\, s_{h1}\, d\Omega + \Delta t \int_\Omega \nabla u_h{}^{i+1} \nabla s_{h1}\, d\Omega + \Delta t \lambda \int_\Omega u^{i+1} s_{h1}\, d\Omega = \Delta t \int_\Omega \lambda (c + (u^i{}_h)^2 v_h)\, s_{h1}\, d\Omega + \int_\Omega u^i{}_h s_{h1}\, d\Omega \\ \int_\Omega (v_h{}^{i+1})\, s_{h2}\, d\Omega + \Delta t \int_\Omega \alpha \nabla v_h{}^{i+1} \nabla s_{h2}\, d\Omega = \Delta t \int_\Omega \lambda (d - (u_h{}^i)^2 v) s_{h2}\, d\Omega + \int_\Omega v_h{}^i s_{h2} d\Omega \\ \forall\, s_{h1}, s_{h2} \in H^1(\Omega) \end{cases} \quad (13)$$

By simplifying we get the following system

$$\begin{bmatrix} J_1{}^{i+1} & +\Delta t\, B_1{}^{i+1} \\ J_2{}^{i+1} & +\Delta t\, B_2{}^{i+1} \end{bmatrix} \begin{bmatrix} u^{i+1} \\ v^{i+1} \end{bmatrix} = \begin{bmatrix} F_1{}^i \\ F_2{}^i \end{bmatrix} + \Delta t \begin{bmatrix} \lambda c \\ \lambda d \end{bmatrix} \quad (14)$$

$$for\ i = 0, 1, 2, 3, \ldots$$

An implicit numerical scheme of Schnakenberg model becomes

$$BU^{i+1} = F^i + \Delta t M \quad (15)$$

Where B is the stiffness matrix, $U = [u_1 v_1, u_2 v_2, \ldots u_n v_n]$, n denotes the nodes on the discrete domain Ω, and M is a vector obtained from a discrete linear form.

3. RESULTS AND DISCUSSIONS

This section presents the main simulation results for the Schnakenberg model. From the methodology section, we obtained an implicit numerical scheme of the Schnakenberg model is as follows:

$$BU^{\,i+1} = F^i + \Delta t\, M$$

Here, B is the stiffness matrix, which is symmetric and positive definite, obtained from the discretization of the symmetrical bilinear form. $U = [u_1 v_1, u_2 v_2, \ldots u_n v_n]$, n indicates nodes on the discrete domain Ω, M is a vector that signifies the estimation of the linear form. The system of algebraic equations obtained from the derived numerical scheme is solved using the conjugate gradient (CG) technique, which is the built-in capability of the Free Fem++ software. By default the tolerance measure of the CG algorithm is $\in = 10^{-1}$. The bi-dimensional bi-directional problem

is solved on a triangular grid, which allows local selection of scaling diffusion parameters. In this model, pattern formations were examined during morphogenesis in the cells of an animal species. The simulations obtained from the derived numerical scheme exhibited stripe- like morphogenesis.

The Numerical results indicate that the reactions-diffusion (RD) equations perform well in describing the features of some biological phenomena in the form of patterns. This study demonstrates the patterns of spots and stripes obtained based on mathematical models. The derived numerical models were tested for various combinations of various choices of scaling diffusion parameters.

For the fixed values of $u^0=1.0, v^0=0.9,\ \lambda=176.72, c=0.1, \alpha=9.1676, d=0.9$ with time step, $\Delta t=0.05$, the solution of equation (15) gives following behaviors at different iterations.

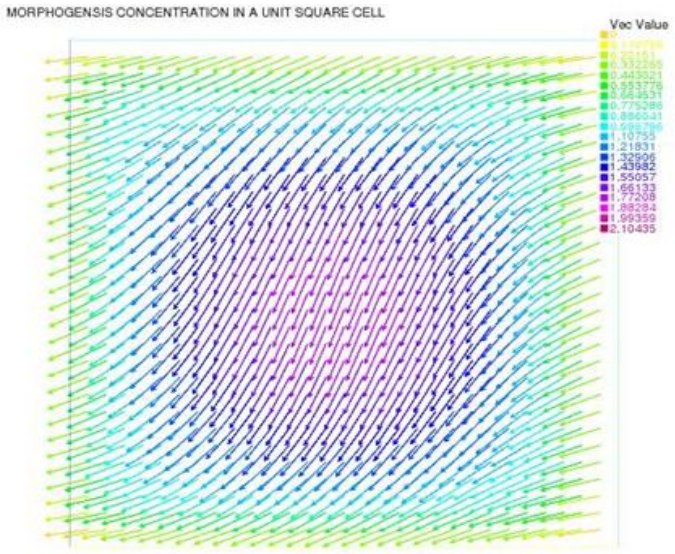

FIGURE 1. A vector plot $[u,v]$ at Second time iteration

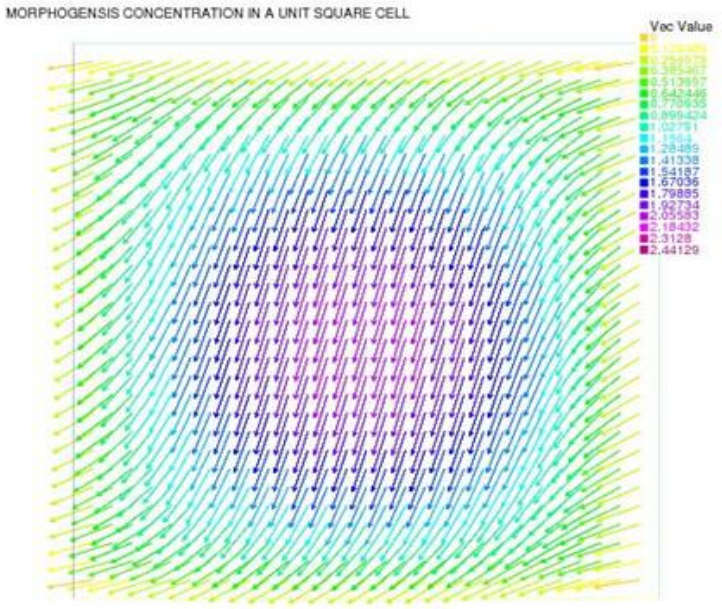

FIGURE 2. A vector plot $[u, v]$ at third time iteration

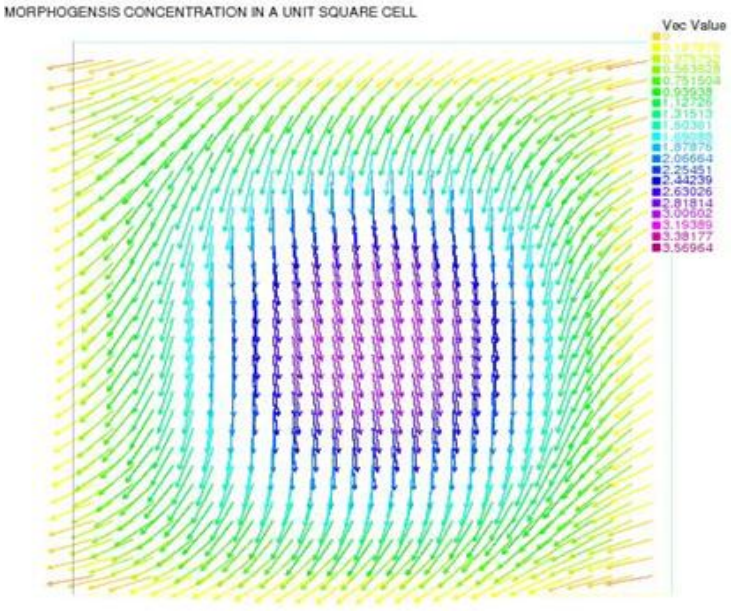

FIGURE 3. A vector plot $[u, v]$ at seventh time iteration

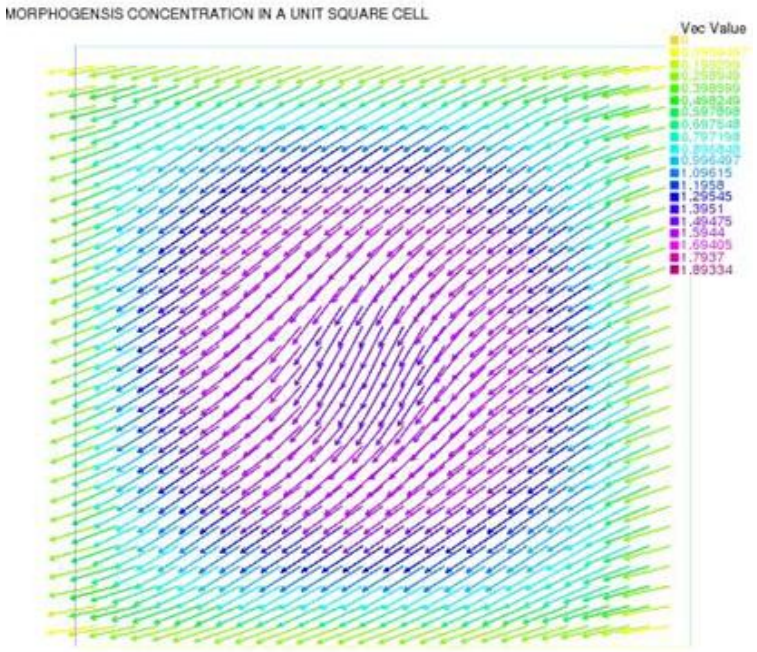

FIGURE 4. A vector plot $[u, v]$ at eighth time iteration

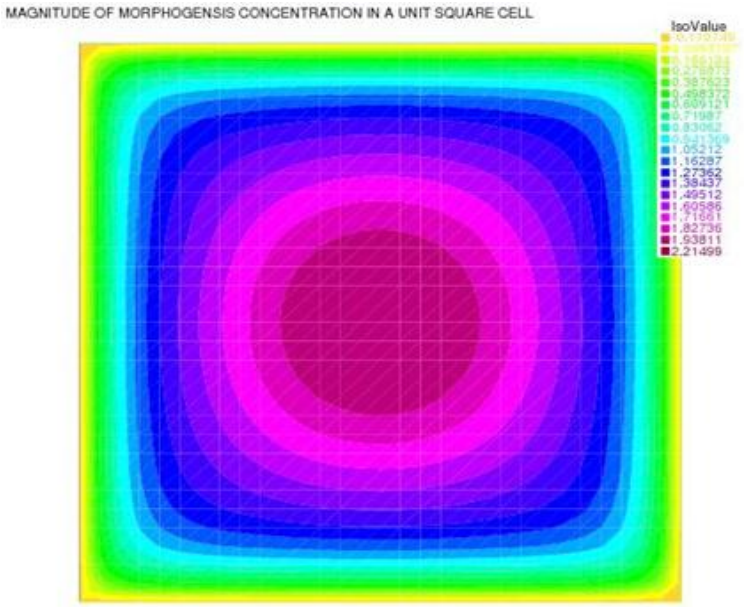

FIGURE 5. Magnitude of [u, v] at second time iteration

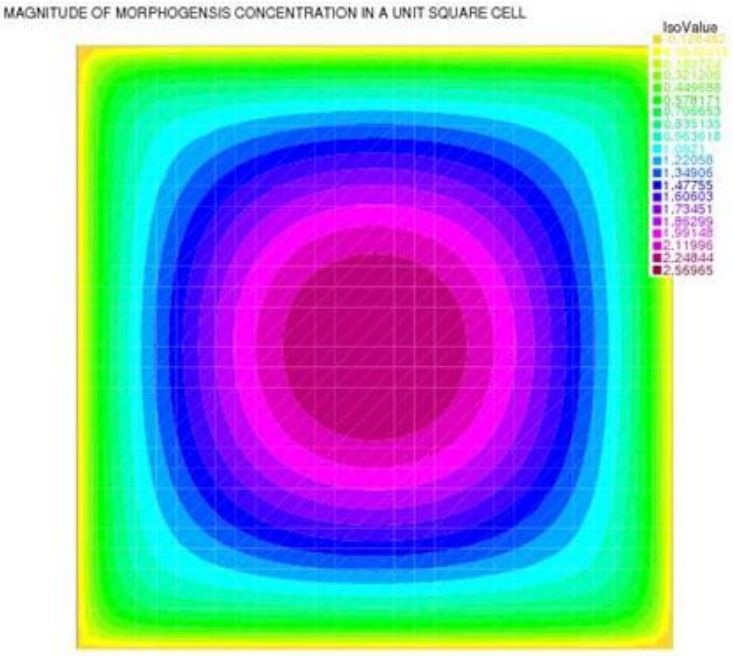

FIGURE 6. Magnitude of [u, v] at third time iteration

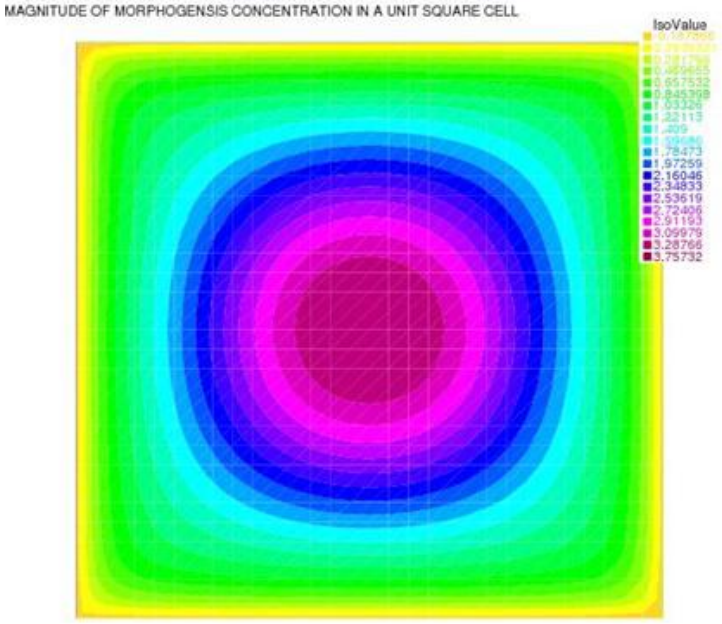

FIGURE 7. Magnitude of [u, v] at seventh time iteration

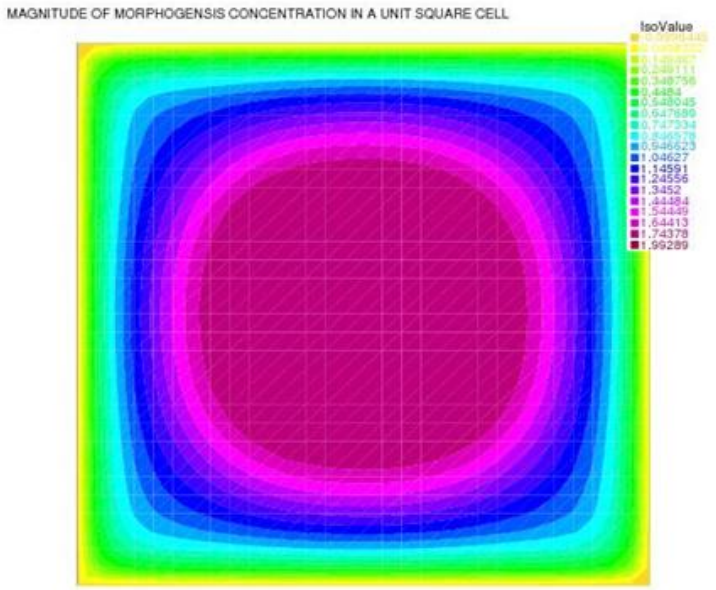

FIGURE 8. Magnitude of [*u*, *v*] at eighth time iteration

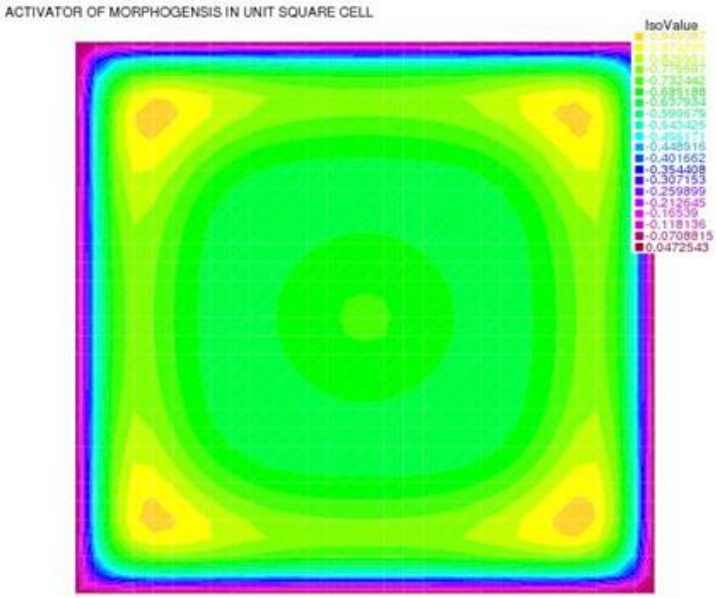

FIGURE 9. The morphogenesis concentration (Activator of [*u*, *v*]) at eight time iteration

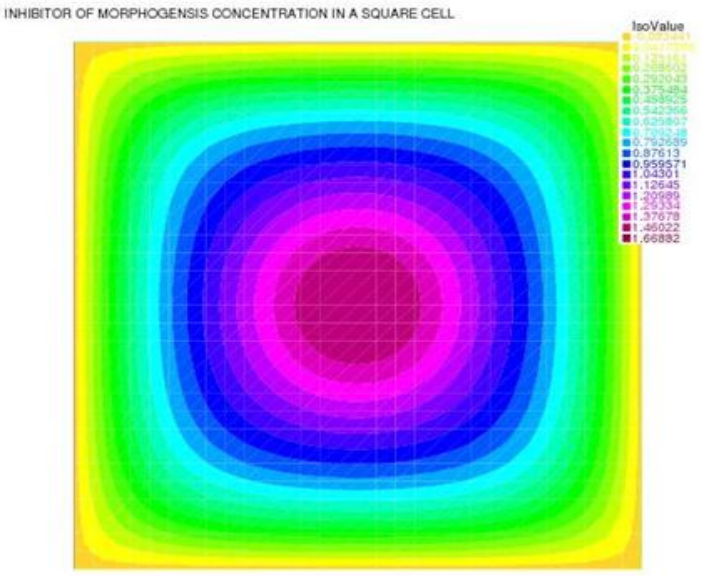

FIGURE 10. The morphogenesis concentration (Inhibitor of [*u*, *v*]) at eighth time iteration

These plots illustrate the solutions to equation (15) with striped and spot like patterns. It was also observed that the chemical concentration increased with time from the boundary towards the center of the cell. An inward direction was observed for the concentration. Additionally, it was observed that the maximum concentrations surround the center of the cell. Figures (1-10) show the chemical concentration inside the cell. The results demonstrate that the reaction-diffusion equations accurately describe the generation of stripe and spot-like patterns that appear on the skin of many animals.

Figures 9 and 10 shows that the activator created spot-like patterns, and inhibitor generated stripe-like patterns in the morphogenesis process. Eight iterations were performed to determine solutions in the morphogenesis process. In implicit numerical models, discrete time steps do not affect the stability of the problem, since implicit numerical models are generally stable.

4. Conclusion and the Future Recommendation

4.1 Conclusion

In this study, an FEM- based implicit numerical scheme was developed to solve the coupled set of nonlinear PDEs. The biological model Schnakenberg was used as the model problem in this

study. The designed implicit numerical schemes were applied to the proposed model problems by using a triangular grid as the discrete domain of the computation. The triangular grid allows the local choice of scaling diffusion parameters. The effects of the various combinations on the local choice of the scaling parameters is an interesting perspective and is shown as a case study for obtaining dense simulation patterns for the chemical concentration in a unit square cell for the animal species. It was observed from the experiments that the obtained simulation patterns were generally the strip- like and spot-like patterns. It is evident from the morphogenesis process that the chemical concentration increases as diffusion proceeds from the boundary to the center. The maximum chemical concentration was observed around the cell center and the minimum at the cell boundary.

The spot-like shapes (non- smooth regions) were seen from the simulation patterns for the activator u in the proposed model; such type of occurring irregularity in the activator process is controlled by the inhibitor v *as* a result of smooth patterns in the form of stripe-like smooth patterns for the chemical concentration. The impact of activator u on the morphogenesis process is a remarkable output for generating spot-like patterns. This regularization perspective which controls the spot-like process using stripe-like smooth combines the proposed models with other methods for the process of pattern formation, such as pigmentation in animals.

In this study, we found that reaction diffusion equations are effective in explaining biological models and estimating pattern formation for chemical processes in cells. The discrete time step choices do not affect the stability of this FEM-based numerical scheme for the coupled set of nonlinear partial differential equations, because the coupled set is implicit, and therefore unconditionally stable.

4.2. Future Recommendation

From the detailed discussion and the observed performance of the numerical implicit scheme discussed in this paper, it is suggested that the developed numerical implicit scheme can be applied to other models for the estimation of the pattern formation for the chemical concentration in animal species. The proposed model, in combination with other biological models for pattern formation in fish, zebras, and other animals, can be used to estimate pattern recognition and

pigmentation processes. The unavailability of exact solutions to the proposed problem does not allow us to indicate a priori error estimates and comparisons with other models or numerical schemes. An a posteriori error estimate is only possible for the proposed problem, which is still a challenging task, especially for nonlinear partial differential (PD) equations. Such error bounds are under consideration for future work.

CONFLICT OF INTERESTS

The authors declare that there is no conflict of interests.

REFERENCES

[1] R.A. Barrio, P.K. Maini, J.L. Aragón, et al. Size-dependent symmetry breaking in models for morphogenesis, Physica D 168–169 (2002), 61–72. https://doi.org/10.1016/S0167-2789(02)00495-5.

[2] M. Bro-Nielsen, Finite element modeling in surgery simulation, Thesis, Technical University of Denmark, 1997.

[3] S.C. Brenner, L.R. Scott, The mathematical theory of finite element methods, Springer, New York, 2008. https://doi.org/10.1007/978-0-387-75934-0.

[4] J. Crampin, Reaction diffusion patterns on growing domains, PhD thesis, University of Oxford, Oxford, 2000.

[5] J. Hoffman, Numerical methods for engineers and scientists, Marcel Dekker Inc, New York, 2001.

[6] A. Madzvamuse, A.J. Wathen, P.K. Maini, A moving grid finite element method applied to a model biological pattern generator, J. Comput. Phys. 190 (2003), 478–500. https://doi.org/10.1016/S0021-9991(03)00294-8.

[7] F.M. Khan, A. Ali, N. Hamadneh, et al. Numerical investigation of chemical Schnakenberg mathematical model, J. Nanomaterials 2021 (2021), 9152972. https://doi.org/10.1155/2021/9152972.

[8] K.S. Al Noufaey, Semi-analytical solutions of the Schnakenberg model of a reaction-diffusion cell with feedback, Results Phys. 9 (2018), 609–614. https://doi.org/10.1016/j.rinp.2018.03.017.

[9] F.M. Khan, A. Ali, Abdullah, et al. Analytical approximation of Brusselator model via LADM, Math. Probl. Eng. 2022 (2022), 8778805. https://doi.org/10.1155/2022/8778805.

[10] E.L. Ince, Ordinary differential equations, Dover, New York, 1956.

[11] C. Chicone, Ordinary differential equations with applications, Springer, New York, 2006.

[12] O. Nikan, Z. Avazzadeh, J.A.T. Machado, Numerical simulation of a degenerate parabolic problem occurring in the spatial diffusion of biological population, Chaos Solitons Fractals 151 (2021), 111220. https://doi.org/10.1016/j.chaos.2021.111220.

[13] N. Muhammad, A. Hakeem, I. Ahmed, et al. Radial basis function neural networks (RBFNN) for secure intrusion detection in the internet of drones (IoD), Proc. Bulg. Acad. Sci. 77 (2024), 1185–1192. https://doi.org/10.7546/CRABS.2024.08.09.

[14] S.B. Tahar, J.J. Muñoz, S.J. Shefelbine, et al.Turing pattern prediction in three-dimensional domains: the role of initial conditions and growth, bioRxiv, (2023). https://doi.org/10.1101/2023.03.29.534782.

[15] A. Gierer, H. Meinhardt, A theory of biological pattern formation, Kybernetik 12 (1972), 30–39. https://doi.org/10.1007/BF00289234.

[16] H.F. Nijhout, A comprehensive model for colour pattern formation in butterflies, Proc. R. Soc. Lond. B Biol. Sci. 239 (1990), 81–113. https://doi.org/10.1098/rspb.1990.0009.

[17] J.C. Vanegas-Acosta, N.S. Landínez, D.A. Garzón-Alvarado, Analysis of Turing instabilities in biological models, Rev. DYNA Univ. Nac. Colomb. Medellin 158 (2009), 123–134.

[18] J.C. Vanegas, N.S. Landínez, D.A. Garzón, Computational solution of biological models of spatial-temporal pattern formation, Ingeniare Rev. Chil. Ing. 17 (2009), 182–194.

[19] I.F. Sbalzarini, Modeling and simulation of biological systems from image data, BioEssays 35 (2013), 482–490. https://doi.org/10.1002/bies.201200051.

[20] K. Page, P.K. Maini, N.A.M. Monk, Pattern formation in spatially heterogeneous Turing reaction–diffusion models, Physica D 181 (2003), 80–101. https://doi.org/10.1016/S0167-2789(03)00068-X.

[21] A.M. Turing, The chemical basis of morphogenesis, Philos. Trans. R. Soc. Lond. B Biol. Sci. 237 (1952), 37–72. https://doi.org/10.1098/rstb.1952.0012.

[22] L. Perko, Differential equations and dynamical systems, Springer, New York 2008.

[23] K.M. Owolabi, Modelling and simulation of a dynamical system with the Atangana-Baleanu fractional derivative, Eur. Phys. J. Plus 133 (2018), 15. https://doi.org/10.1140/epjp/i2018-11863-9.

[24] K. Alligood, T. Sauer, C.J. Yorke, An introduction to dynamical systems, Springer, New York, 1997.

[25] A. Katok, B. Hasselblatt, Introduction to the modern theory of dynamical systems, Cambridge University Press, 1995. https://doi.org/10.1017/CBO9780511809187.

[26] M.W. Hirsch, S. Smale, Differential equations, dynamical systems, and linear algebra, Academic Press, San Diego, (1989).

[27] S. Singh, Numerical investigation of wave pattern evolution in Gray–Scott model using discontinuous Galerkin finite element method, in: Advances in Mathematical and Computational Modeling of Engineering Systems, 1st ed., CRC Press, Boca Raton, 2023: pp. 47–58. https://doi.org/10.1201/9781003367420-2.

[28] A. Tok-Onarcan, N. Adar, I. Dag, Wave simulations of Gray-Scott reaction-diffusion system, Math. Methods Appl. Sci. 42 (2019), 5566-5581. https://doi.org/10.1002/mma.5534.

[29] H. Che, Y.L. Wang, Z.Y. Li, Novel patterns in a class of fractional reaction–diffusion models with the Riesz fractional derivative, Math. Comput. Simul. 202 (2022), 149–163. https://doi.org/10.1016/j.matcom.2022.05.037.

[30] M. Alqhtani, K.M. Owolabi, K.M. Saad, E. Pindza, Efficient numerical techniques for computing the Riesz fractional-order reaction-diffusion models arising in biology, Chaos Solitons Fractals 161 (2022), 112394. https://doi.org/10.1016/j.chaos.2022.112394.

[31] S.M. Hussain, R. Mahat, N.M. Katbar, et al. Artificial neural network modeling of mixed convection viscoelastic hybrid nanofluid across a circular cylinder with radiation effect: Case study, Case Stud. Therm. Eng. 50 (2023), 103487. https://doi.org/10.1016/j.csite.2023.103487.

[32] H. Ali, N.G. Trisha, M.S. Islam, Galerkin-Bernstein approximations of the system of time dependent nonlinear parabolic PDEs, preprint, (2023). https://doi.org/10.48550/arXiv.2307.04581.

[33] R.C. Mittal, S. Kumar, R. Jiwari, A cubic B-spline quasi-interpolation algorithm to capture the pattern formation of coupled reaction-diffusion models, Eng. Comput. 38 (2022), 1375–1391. https://doi.org/10.1007/s00366-020-01278-3.

[34] M. Youssouf, B. Moussa, P. Youssouf, Resolution of the standard telegraph equation by the Laplace-Adomian method, J. Adv. Math. Comput. Sci. 39 (2024), 63–71. https://doi.org/10.9734/jamcs/2024/v39i21868.

[35] S. Jafari Nivlouei, M. Soltani, J. Carvalho, et al. Multiscale modeling of tumor growth and angiogenesis: evaluation of tumor-targeted therapy, PLOS Comput. Biol. 17 (2021), e1009081. https://doi.org/10.1371/journal.pcbi.1009081.

[36] A. Hakeem, N.M. Katbar, F. Muhammad, et al. QSPR analysis of some important drugs used in heart attack treatment via degree-based topological indices and regression models, Polycycl. Aromat. Compd. 44 (2024), 5237–5246. https://doi.org/10.1080/10406638.2023.2262697.

[37] A. Hakeem, N.M. Katbar, F. Muhammad, N. Ahmed, On the molecular structure modelling of gamma graphyne and armchair graphyne nanoribbon via reverse degree-based topological indices, Mol. Phys. 122 (2024), e2259510. https://doi.org/10.1080/00268976.2023.2259510.

[38] S.M. Hussain, R. Parveen, N.M. Katbar, et al. Entropy generation analysis of MHD convection flow of hybrid nanofluid in a wavy enclosure with heat generation and thermal radiation, Rev. Adv. Mater. Sci. 63 (2024), 20240037. https://doi.org/10.1515/rams-2024-0037.

[39] O.C. Zienkiewicz, R.L. Taylor, The finite element method for solid and structural mechanics, Elsevier, 2005.

[40] R.A. Adams, J.J.F. Fournier, Sobolev spaces, Academic Press, Amsterdam, 2003.

[41] K.B. Amur, Contrôle adaptatif, techniques de régularisation et applications en analyse d'images, PHD thesis LMAM University of Metz, France, 2011.

[42] K.B. Amur, Some regularization strategies for ill-posed denoising problem, Int. J. Tomogr. Stat. 19 (2012), 46-59.

[43] K.B. Amur, A posteriori control of regularization for complementary image motion problem, Sindh Univ. Res. J. Sci. Ser. 45 (2013), 546-552.

[44] K.B. Amur, Local and adaptive control of regularization for some nonlinear variational models in image motion, in: Fifth international conference on Scientific Computing and Partial differential Equations SPDE-14, Hong Kong, 2014.